BMJ Open Ophthalmology

Anti-inflammatory actions of ripasudil ameliorate experimental autoimmune uveoretinitis in the acute phase

Kozo Harimoto,[1] Yoshiaki Nishio,[1] Hideaki Someya,[1] Tomohito Sato,[1] Masataka Ito,[2] Masaru Takeuchi [1]

To cite: Harimoto K, Nishio Y, Someya H, *et al*. Anti-inflammatory actions of ripasudil ameliorate experimental autoimmune uveoretinitis in the acute phase. *BMJ Open Ophthalmology* 2025;**10**:e001981. doi:10.1136/bmjophth-2024-001981

► Additional supplemental material is published online only. To view, please visit the journal online (https://doi.org/10.1136/bmjophth-2024-001981).

Received 4 October 2024
Accepted 8 February 2025

[1]Department of Ophthalmology, National Defense Medical College, Tokorozawa, Saitama, Japan
[2]Developmental Anatomy and Regenerative Biology, National Defense Medical College, Tokorozawa, Saitama, Japan

Correspondence to
Professor Masaru Takeuchi; masatake@ndmc.ac.jp

ABSTRACT

Introduction Rho-associated protein kinases (ROCKs) are a key regulator of T cell function, influencing a wide range of processes from activation to differentiation. Experimental autoimmune uveoretinitis (EAU) is an animal model of human non-infectious uveitis. This study aimed to evaluate the suppressive effects of ripasudil, a ROCK inhibitor, on ocular inflammation when administered from the onset of EAU and to elucidate the underlying mechanisms of its inhibitory effects.

Methods EAU was induced in wild-type C57BL/6 mice by immunisation with IRBP peptide. Ripasudil or its vehicle, PBS, was intraperitoneally administered daily starting from 8 days post-immunisation. Clinical and histopathological examinations and analysis of T cell activation state were conducted. In addition, T cell gene expression profiles in the relevant immune functions were identified using single-cell RNA sequencing (scRNA-seq).

Results The development of EAU was significantly attenuated and T cell activation and Th1 cell differentiation were significantly inhibited in mice with ripasudil (RIP-EAU) compared with mice with PBS (PBS-EAU), scRNA-seq using splenic T cells indicated that genes involved in the ROCK signalling pathway were highly expressed in low-differentiated Th1/Th17 cells, intermediate Th1 cells and differentiated Th1 cells. In addition, although differentiated Th1 and Th17 cells constituted similar proportions between PBS-EAU and RIP-EAU mice, RIP-EAU mice exhibited fewer low-differentiated Th1/Th17 cells and intermediate Th1 cells compared with PBS-EAU mice.

Conclusion Ripasudil suppressed EAU when administered from the onset of the disease by inhibiting cells that strongly express genes involved in the ROCK signalling pathway and differentiate into Th1 cells.

WHAT IS ALREADY KNOWN ON THIS TOPIC

⇒ Ripasudil is an inhibitor of Rho-associated protein kinase which controls the cytoskeleton and acts on cell morphology, movement and adhesion. It has been reported to suppress an animal model of uveitis caused by innate immunity, but its inhibitory effect on uveitis induced mainly by acquired immunity via T cells has not been demonstrated.

WHAT THIS STUDY ADDS

⇒ Ripasudil inhibited T-cell-mediated uveitis by administration from the effector phase.

HOW THIS STUDY MIGHT AFFECT RESEARCH, PRACTICE OR POLICY

⇒ Ripasudil is already used as an eye drop to treat glaucoma. Our current findings suggest the potential of ripasudil through drug repositioning in the treatment of non-infectious uveitis.

INTRODUCTION

Uveitis is a sight-threatening inflammatory disease that affects the uvea and retina and is estimated to be responsible for up to 10% of all causes of blindness.[1] Uveitis aetiologically classified into infectious and non-infectious.[2] In non-infectious uveitis, autoimmunity and autoinflammatory components are thought to be involved in the pathogenesis.[3]

Experimental autoimmune uveoretinitis (EAU) is an animal model of non-infectious uveoretinitis that is widely used to study the pathogenesis and investigate effective therapies for the disease. The development of EAU is dependent on the activation of T cells, in which Th1 and Th17 cells, secreting inflammatory cytokines, such as IFN-γ and IL-17, promote the inflammation and destruction of ocular tissue,[4 5] while T regulatory (T reg) cells contribute to amending the disease.[6–8]

The Rho family of small GTPase proteins controls the cytoskeleton and acts on cell morphology, movement and adhesion.[9] Notably, Rho GTPases activate downstream signalling cascades through serine/threonine kinases called Rho-associated protein kinases (ROCKs).[10] It has been reported that ROCK inhibitors effectively diminish the production of inflammatory cytokines by T cells,[11 12] differentiation of Th1 and Th17 cells,[13] and animal models of autoimmune diseases.[11 14 15] Ripasudil is a ROCK inhibitor suppressing the transfer of the terminal phosphate from ATP to their substrates and is the first Rho-kinase inhibitor ophthalmic solution developed for the treatment of glaucoma and ocular hypertension in Japan in 2014.[16]

In endotoxin-induced uveitis (EIU), an acute ocular inflammation mediated by injection of lipopolysaccharide, ripasudil suppressed infiltrating cells and protein extravasation in the aqueous humour and reduced the numbers of infiltrating cells in the iridociliary body and adherent leukocytes in retinal blood vessels.[17] These effects were mediated by suppression of ICAM-1 and MCP-1 expression, as well as TNF-α/NF-κB inhibition in macrophages.

Corticosteroids and immunomodulatory agents such as cyclosporine are effective for treatment of non-infectious uveitis; however, some cases remain refractory to these treatments. Biological agents, such as anti-TNFα drugs, are used for these cases,[18] but are costly, imposing a substantial financial burden on both patients and healthcare systems. In addition, while these drugs have been presented to suppress uveitis in EAU models,[19] this effect was observed when the drugs were administered from the induction phase, prior to the onset of uveitis, immediately after immunisation. In light of the potent anti-inflammatory effects of ripasudil observed in EIU, we investigated in this study whether ripasudil administration from the induction phase of EAU would be effective in reducing the ocular inflammation and the mechanisms underlying its inhibitory effects.

MATERIALS AND METHODS

Animals

Female wild-type C57BL/6N mice, aged 8–9 weeks old, were purchased from Japan SLC (Shizuoka, Japan). All mice were housed in the Center for Laboratory Animal Science of the National Defense Medical College under specific pathogen-free conditions with a regular light-dark cycle (14 hours of light and 10 hours of darkness per day) and access to food and water ad libitum.

EAU induction

Mice were immunised subcutaneously in the neck region with 200 µg of human IRBP 1–20 (hIRBP-p) emulsified in 0.2 mL of complete Freund's adjuvant (Difco, Detroit, Michigan, USA) containing 1 mg of *Mycobacterium tuberculosis* strain H37Ra (Difco). As an additional adjuvant, 0.5 µg of pertussis toxin (Sigma Aldrich, St. Louis, Missouri, USA) in 0.2 mL of PBS was injected intraperitoneally.

Ripasudil and PBS administration

From day 8 after immunisation, 200 µL of 5 mg/mL ripasudil in PBS was administered intraperitoneally to each mouse in the ripasudil (RIP-EAU) group, and 200 µL of PBS was administered intraperitoneally to each mouse in the PBS (PBS-EAU) group daily until day 20. Ripasudil dosage was determined with reference to a previous report.[17]

Clinical and optical coherence tomography scoring

Clinical and optical coherence tomography (OCT) scoring of EAU was evaluated on days 14 and 21 post-immunisation, using a Micron IV fundus camera with MICRON Image-Guided OCT (Phoenix Research Labs, Pleasanton, California, USA). EAU severity of both clinical and OCT was graded on a scale of 0–4 according to the previous report.[20]

Histological scoring

Histological study was conducted on days 14 and 21 post-immunisation. The mice were deeply anaesthetised with pentobarbital (Kyoritsu, Tokyo, Japan) and isoflurane (Wako, Osaka, Japan), and perfused with 4% paraformaldehyde phosphate buffer solution (Wako) for fixation. The eyes were collected and fixed in the same fixative overnight at 4°C and embedded in paraffin. Sections of 5 µm thickness were prepared and stained with H&E. Severity of ocular inflammation was scored on a scale of 0–4 according to the previous report.[20]

Flow cytometry

Spleens from PBS-EAU and RIP-EAU mice were harvested on day 21 post-immunisation and homogenised. Cells were incubated with anti-mouse CD16/CD32 (eBioscience, Waltham, Massachusetts, USA) to block Fc receptors before staining. For detection of activated T cells in the spleen, the cells were stained with CD3-APC/Cyanine7 (clone:17A2, BioLegend, San Diego, California, USA), CD4-APC (clone: RM4-5), CD44-FITC (clone: IM7) and CD62L-PE (clone: W18021D) antibodies. For intracellular staining, cells were stimulated with 50 ng/mL phorbol 12-myristate 13-acetate (PMA; Sigma-Aldrich, St. Louis, Missouri, USA) and 0.5 µg/mL ionomycin (Sigma-Aldrich) in the presence of 10 µg/mL brefeldin A (Sigma-Aldrich) for 4 hours at 37°C, then collected and stained with CD3-Pacific Blue (clone 17A2) and CD4-PerCP/Cyanine5.5 (clone GK1.5). Subsequently, cells were fixed and permeabilised using a permeabilisation/fixation buffer (Becton Dickinson Bioscience, Franklin Lakes, New Jersey, USA) according to the manufacturer's protocol, followed by incubation with IFN-γ-APC (clone XMG1.2) or IL-17A-APC (clone TC11-18H10.1) antibodies. For Foxp3 staining, cells were stained with CD3-APC/Cyanine7 and CD4-APC antibodies, followed by fixation and permeabilisation using a Foxp3/Transcription Factor Staining Buffer Set (eBioscience) and stained with Foxp3-Brilliant Violet 421 (clone MF-14) antibody. The cells were analysed by FACSCanto II Flow Cytometer (BD), and the data were processed by CellQuest software (BD). The gating strategies are shown in online supplemental figure S1–S3.

Single-cell RNA sequencing

Sample preparation

On day 21 post-immunisation, the mice were anaesthetised, and their spleens were obtained. To enhance the purity of T cells, the spleen cell suspension was sorted using the magnetic-activated cell sorting cell separator system with the Pan T cell isolation kit (Miltenyi Biotec, Bergisch Gladbach, Germany).

scRNA-seq data processing

The cell suspension was loaded onto Chromium microfluidic chips with 3' chemistry and barcoded using a 10× Chromium Controller (10× Genomics, Pleasanton, California, USA). The RNA from the barcoded cells was then reverse-transcribed and sequencing libraries were constructed using reagents from a Chromium Single Cell 3'reagent v2 kit (10× Genomics) according to the manufacturer's instructions. Sequencing was performed on NovaSeq6000 PE150 (Illumina) according to the manufacturer's instructions at Novogene. Reads from scRNA-seq were processed by Cell Ranger software V.7.0.0 (10× Genomics) with the default parameters for each sample separately. scRNA-seq data analyses were performed by R package Seurat V.4.3.0.[21] First, low-quality cell data were excluded. All samples were integrated using the 'anchor' method, and dimensional reduction was performed using principal component analysis. Then, uniform manifold approximation and projection (UMAP) plot was generated using PC1–PC20. These single-cell profiles were clustered by shared nearest neighbour modularity optimisation (resolution=0.5) and projected on the UMAP plot. Highly expressed genes characterising each cluster ($p<0.05$, Log_2 FC>0.25) were identified by Seurat Find All Markers, and enrichment analysis was performed using R package cluster Profiler V.4.2.2 based on Reactome Pathway database (R package ReactomePA V.1.38.0) and Gene Ontology database (R package org.Mm.eg.db V.3.14.0).

Statistical analyses

Statistical analyses were performed using JMP Pro V.15 (SAS Institute). Wilcoxon rank-sum test was used for statistical analyses of the clinical score, OCT score, histological score and proportions of naïve T cells, activated T cells, IFN-γ-producing or IL-17A-producing $CD4^+$ T cells, and Treg cells. P values less than 0.05 were considered significant.

RESULTS

Improvement of experimental autoimmune uveitis (EAU) in mice treated with ripasudil

We first investigated whether ripasudil administration via intraperitoneal injection starting from day 8 post-immunisation with hIRBP-p inhibited the progression of EAU.

Figure 1 shows colour fundus images of EAU in mice administered PBS (PBS-EAU group) or ripasudil (RIP-EAU group) 14 and 21 days after hIRBP-p immunisation. EAU was observed in all mice in both groups, but the mean clinical score of EAU was significantly higher in PBS-EAU mice than in RIP-EAU mice both on days 14 and 21 (figure 1A). Representative colour fundus images show multiple retinal exudates and extensive retinal

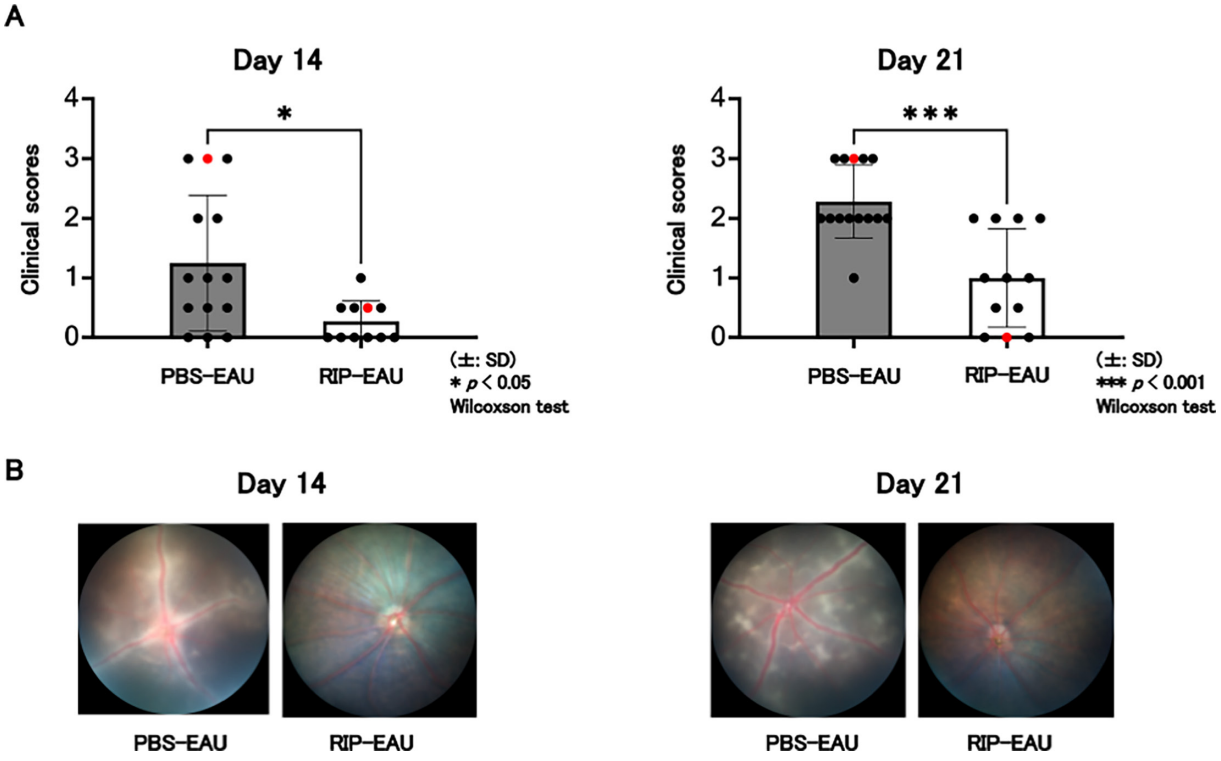

Figure 1 Clinical investigation of PBS-EAU and RIP-EAU mice. (A) Bar graphs show the clinical scores in PBS-EAU and RIP-EAU mice at days 14 and 21 post-immunisation (n=12 eyes in each group). Each plot represents the clinical score for each eye. *p<0.05, ***p<0.001 determined using Wilcoxon test. (B) Colour fundus images of the eyes with the red-highlighted plots are shown for the PBS-EAU and RIP-EAU mouse groups. Data are representative of three independent experiments with similar results. RIP-EAU, ripasudil-experimental autoimmune uveoretinitis.

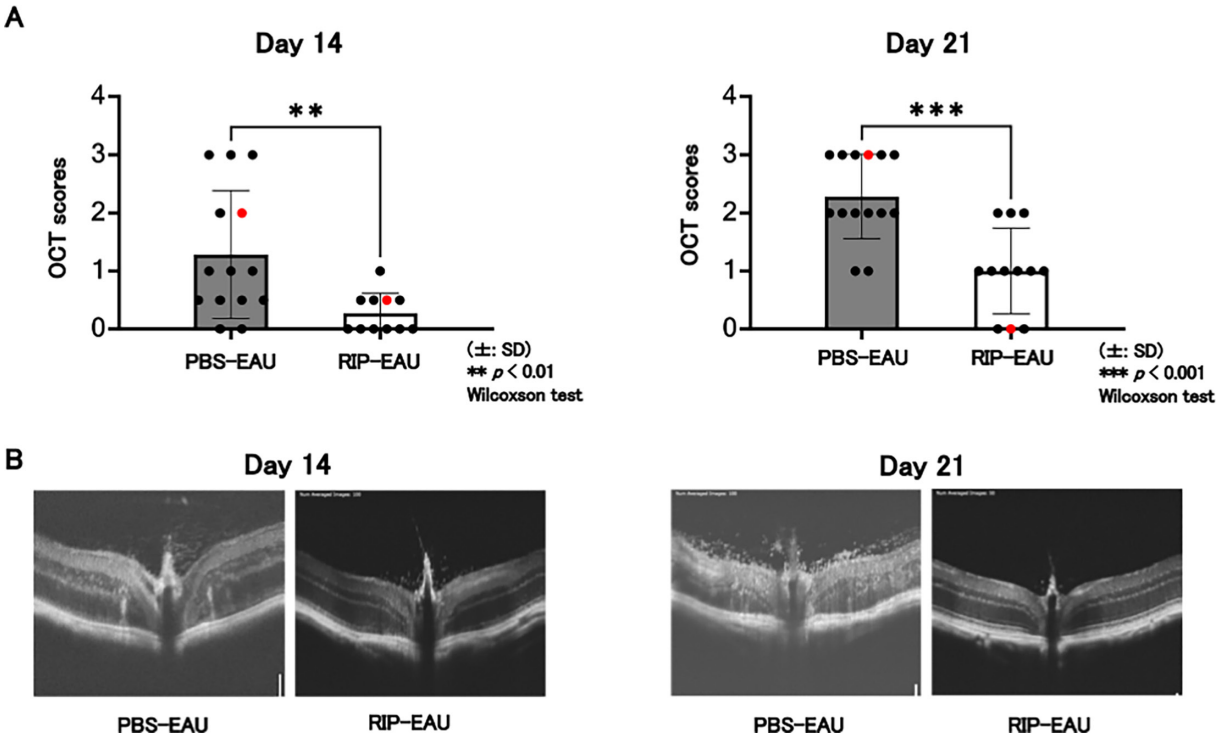

Figure 2 OCT evaluation of PBS-EAU and RIP-EAU mice. (A) Bar graphs show the OCT scores in PBS-EAU and RIP-EAU mice at days 14 and 21 post-immunisation (n=12 eyes in each group). Each plot represents the OCT score for each eye. **p<0.01, ***p<0.001 determined using Wilcoxon test. (B) OCT scans of the eyes with the red-highlighted plots are shown for the PBS-EAU and RIP-EAU mouse groups. Data are representative of three independent experiments with similar results. OCT, optical coherence tomography; RIP-EAU, ripasudil-experimental autoimmune uveoretinitis.

vasculitis on day 14, and increased retinal exudates on day 21 in a PBS-EAU mouse (figure 1B). On the other hand, multiple retinal exudates and extensive retinal vasculitis were much milder in an RIP-EAU mouse compared with a PBS-EAU mouse on both days 14 and 21.OCT images of PBS-EAU and RIP-EAU mice on days 14 and 21 after immunisation with hIRBP-p are displayed in figure 2. Mean OCT score of EAU was significantly higher in PBS-EAU mice than in RIP-EAU mice both on days 14 and 21 (figure 2A). Representative OCT image of the eye of a PBS-EAU mouse showed numerous vitreous infiltrating cells near the retinal surface, papillary oedema, destruction of retinal layer structure due to infiltrating cells, and granuloma-like lesions on day 14, which worsened on day 21 (figure 2B). OCT images of the eye of an RIP-EAU mouse showed only mild cell infiltration in the vitreous and the retina. Similar to these findings, the mean histopathological score was significantly higher in PBS-EAU mice compared with RIP-EAU mice, which was consistent with the OCT images (figure 3A). Representative histopathology of PBS-EAU mice showed extensive cellular infiltration into the vitreous and all retinal layers, disruption of retinal layer structure and granuloma-like lesions, whereas RIP-EAU mice exhibited only mild cellular infiltration in the vitreous and retina with preservation of retinal lamination (figure 3B).

T cell states and proportions of Th1, Th17 and regulatory T (Treg) cells in EAU-induced mice treated with ripasudil

T cell activation is essential for EAU progression, and Th1 and Th17 cells play an important role in the pathogenesis of EAU,[4] while Treg cells are involved in the remission.[22] Figure 4 shows the expression of CD44 and CD62L among $CD3^+CD4^+$ T cells and the proportions of Th1, Th17 and Treg cells in the spleen of PBS-EAU and RIP-EAU mice. Naïve T cells with the $CD44^-CD62L^+$ phenotype were slightly greater in RIP-EAU mice compared with PBS-EAU mice, although the difference was not statistically significant. In contrast, activated T cells with the $CD44^+CD62L^-$ phenotype were significantly lower in RIP-EAU mice than in PBS-EAU mice (figure 4A,B). The mean proportion of Th1 cells with the $CD4^+IFN\text{-}g^+$ phenotype was significantly greater in PBS-EAU mice (13.3%±2.1%) than in RIP-EAU mice (8.2%±1.5%) (figure 4C), while the proportions of Th17 cells with the $CD4^+IL\text{-}17^+$ phenotype and Treg cells with the $CD4^+Foxp3^+$ phenotype were comparable between PBS-EAU mice (4.8%±1.1% and 1.1%±0.8%) and RIP-EAU mice (4.4%±0.9% and 0.9%±0.5%) (figure 4D,E).

Identification of transcriptional changes in EAU-induced mice treated with ripasudil by scRNA-seq

In order to elucidate the potential signalling mechanisms underlying the inhibition of EAU in RIP-EAU mice, splenic T cells extracted from PBS-EAU and RIP-EAU

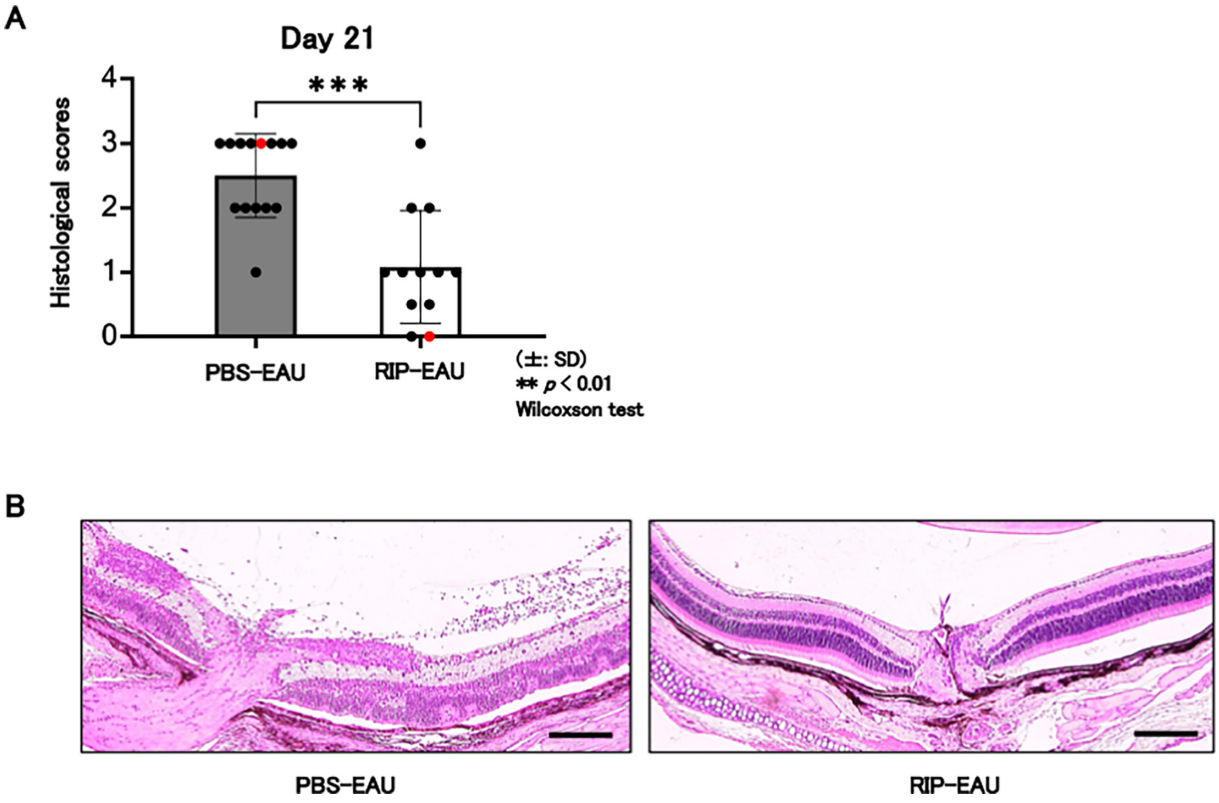

Figure 3 Histopathological evaluation of PBS-EAU and RIP-EAU mice (A) Bar graphs show the in PBS-EAU and RIP-EAU mice at days 14 and 21 post-immunisation (n=12 eyes in each group). Each plot represents the OCT score for each eye. ***p<0.001 determined using Wilcoxon test. (B) Histological sections of the eyes with the red-highlighted plots are shown for the PBS-EAU and RIP-EAU mouse groups. Scale bars: 100 µm. Data are representative of three independent experiments with similar results. OCT, optical coherence tomography; RIP-EAU, ripasudil-experimental autoimmune uveoretinitis.

mice on day 21 post-immunisation with hIRBP-p were applied for scRNA-seq analysis. As shown in figure 5A, UMAP clustering plot of whole $CD3^+$ cells obtained from 4 PBS-EAU and RIP-EAU mice were annotated to naïve $CD4^+$ T cells, low-differentiated Th1+Th17 cells, intermediate-differentiated Th1 cells, full-differentiated Th1 cells, full-differentiated Th17 cells, Treg cells, naïve $CD8^+$ T cells and $CD8^+$ cells (CTL) based on marker genes (insulin-like growth factor binding protein 4 (IGFBP4), CCR7, IFN-g, CCR5, CXCR3, IL-17A, IL-17F, RAR-related orphan receptor C (RORC), STAT3, IL-23R, IRF4, CCR6, Foxp3, CTLA4, TNFRSF18 (GITR), TGFb, TIGIT and CD8a).[23 24] As shown in figure 5B, the proportions of both naïve CD4_2 T cells expressing $IGFBP4^{high}$ and naïve CD8_1 T cells expressing $CD8a^{high}$ and $CCR7^{low}$ were lower in PBS-EAU mice than in RIP-EAU mice, suggesting that activation and differentiation of naïve T cells classified into these clusters were suppressed by the administration of ripasudil. The proportions of low-differentiated Th1 cells expressing IFN-γ^{middle}, T-bet^{middle}, $STAT4^{low}$, $CXCR3^{low}$ and $CCR5^{middle}$ within the Th1/Th17 cell cluster, intermediate-differentiated Th1 cells expressing IFN-γ^{middle}, T-bet^{high}, $STAT4^{high}$, $CXCR3^{low}$, and $CCR5^{high}$, and low-differentiated Th17 cells expressing $RORC^{low}$, IL-$23R^{middle}$, $IRF4^{low}$, and $CCR6^{middle}$ within the Th1/Th17 cell cluster were lower in RIP-EAU mice than in PBS-EAU mice, suggesting that differentiation into Th1 and Th17 cells was suppressed by the administration of ripasudil. In addition, the proportions of Treg cells expressing $Foxp3^{high}$, $CTLA4^{high}$, $GITR^{high}$, $TGFb^{low}$ and $TIGIT^{low}$ and CTL expressing $CD8a^{middle}$, T-bet^{low}, $STAT4^{middle}$, and $CXCR3^{low}$ were also less in RIP-EAU mice compared with PBS-EAU mice. On the other hand, the populations of full-differentiated Th1 cells expressing IFN-γ^{high}, T-bet^{middle}, $STAT4^{low}$, $CXCR3^{high}$ and $CCR5^{high}$ and full-differentiated Th17 cells expressing IL-17A-^{high}, IL-$17F^{middle}$, $RORC^{high}$, $STAT3^{low}$, IL-$23R^{high}$, $IRF4^{low}$ and $CCR6^{middle}$ in RIP-EAU mice were not lower in RIP-EAU mice than in PBS-EAU mice. Subsequently, we performed enrichment pathway analysis for each cluster to investigate the involvement of the RHO-associated signalling pathway (online supplemental file 1). Figure 5C shows the involvement of the RHO-associated signalling pathway in low-differentiated Th1/Th17, intermediate-differentiated Th1, full-differentiated Th1, full-differentiated Th17 and Treg cell clusters compared with other clusters. The RHO-associated signalling pathway was extensively involved in the low-differentiated Th1/Th17 cluster, followed by the intermediate-differentiated Th1 cluster and the full-differentiated Th1 cluster, with less involvement in the full-differentiated Th17 and Treg cell clusters. No significant expression of the RHO-associated signalling pathway was observed in naïve CD4, naïve CD8 or CTL cells.

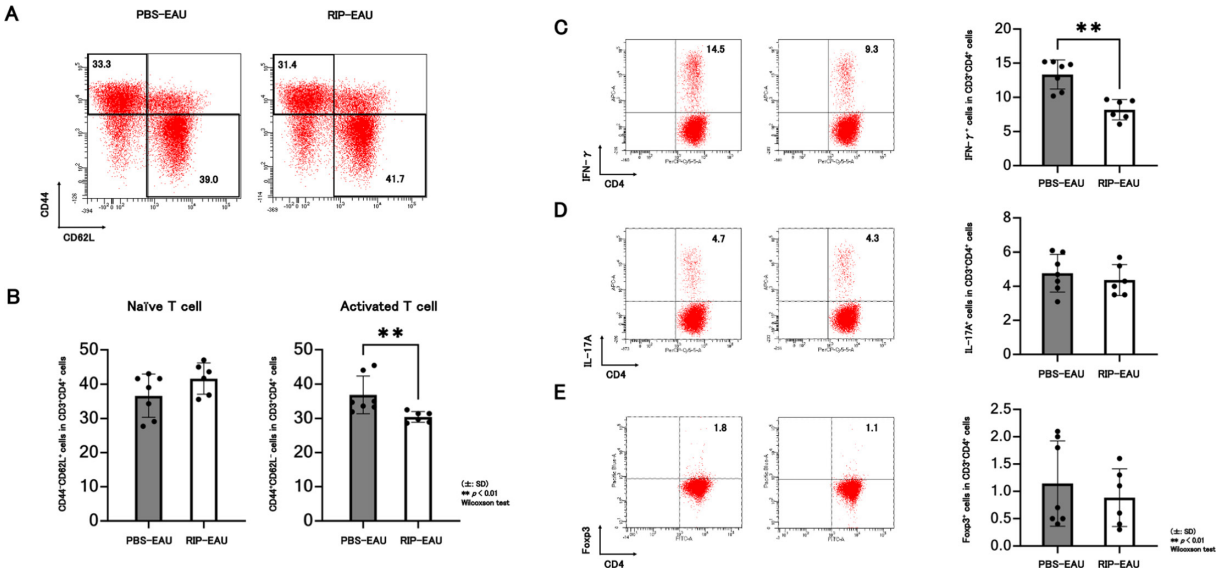

Figure 4 T cell activation and polarisation in the spleen of PBS-EAU and RIP-EAU mice Spleen cells were obtained from PBS-EAU and RIP-EAU mice at days 21 post-immunisation and analysed for T cell subsets by flow cytometry. (A) Representative dot plot data of $CD62L^+$ $CD44^+$ cells. (B) Bar graphs show the proportions of $CD44^-CD62L^+$ (naïve) cells and $CD44^+CD62L^-$ (activated) cells in $CD3^+CD4^+$ T cells. Each plot represents the proportion for each mouse. (C–E) Representative dot plot data from one mouse in each group and bar graphs show the proportions of IFN-γ^+CD4^+ T (Th1) cells (C), IL-$17A^+CD4^+$ T cells (Th17) cells (D), and $Foxp3^+CD4^+$ T (Treg) cells (E) in $CD3^+CD4^+$ T cells (n=6 mice in each group). Each plot represents the proportion for each mouse. **p<0.01 determined using Wilcoxon test. Data are representative of three independent experiments with similar results. RIP-EAU, ripasudil-experimental autoimmune uveoretinitis.

DISCUSSION

The present study indicated that ripasudil administration initiated from the effector phase of EAU, significantly reduced both the incidence and severity of the disease, as assessed clinically and histopathologically.

$CD44^+CD62L^-$ activated T cells were significantly more and $CD44^-CD62L^+$ naive T cells were significantly less in the spleen of RIP-EAU mice compared with PBS-EAU mice. While the proportions of cells in the naive CD4_1 and naive CD8_2 clusters were comparable between PBS-EAU and RIP-EAU mice according to scRNA-seq analysis, the proportions of cells in the naive CD4_2 and naive CD8_1 clusters were greater in RIP-EAU mice than in PBS-EAU mice, suggesting that T cell differentiation in these populations may have been suppressed.

The dynamic balance between the effector Th1/Th17 and Treg cells regulates the development of EAU.[4 6–8 25] Experimental autoimmune encephalomyelitis (EAE) is an animal model of multiple sclerosis.[26] Similarly, EAE is characterised by inflammation mediated by Th1/Th17 cells and suppressed by Treg cells.[26] Fasudil, a ROCK inhibitor developed before ripasudil, prevented the development of EAE accompanied by a reduction of IFN-g and IL-17 production by T cells.[14] In addition, encephalomyelitic T cells isolated from EAE-induced mice were co-cultured with fasudil-treated microglia, revealing a decrease in the frequency of Th17 cells and IL-17 production, while the frequency of Treg cells and IL-10 production increased.[27] These findings suggest that fasudil may induce a shift in the phenotype of encephalomyelitic T cells from Th17 to Treg. FaD-1, is a fasudil derivative, also ameliorates the neurological defects and the severity of EAE, accompanied by inhibition of Th1 and Th17 responses in the spinal cord of mice developing EAE.[28] In contrast, our study found that the frequency of IFN-γ-producing Th1 cells in the spleen was significantly suppressed in RIP-EAU compared with PBS-EAU, however, neither suppression of IL-17-producing Th17 cells nor increase of Treg cells based on Foxp3 expression was observed. Since scRNA-seq analysis using splenic T cells revealed that ROCK signalling pathway-related genes were highly expressed in low-differentiated Th1/Th17 cells, intermediate-differentiated Th1 cells, and full-differentiated Th1 cells, but were low in full-differentiated Th17 cells. In addition, the populations of low-differentiated Th1/Th17 cells and intermediate-differentiated Th1 cells were lower in RIP-EAU mice compared with PBS-EAU mice, suggesting that Th1 progenitor cells may be more sensitive to the suppression by ripasudil than Th17 progenitor cells. However, the unchanged proportions of full-differentiated Th1 and Th17 cells between PBS-EAU and RIP-EAU mice indicate that ripasudil may have limited effects on these fully differentiated cell populations. On the other hand, since expression of ROCK signalling pathway-related genes was also observed in the Treg cells, the lack of increased Treg cells following ripasudil administration, despite differing from EAE reports, was likely an expected consequence.

ROCK signalling pathway-related genes were expressed greater in full-differentiated Th1 cells than in full-differentiated Th17 cells. Since Th17 cells bridge innate and adaptive immunity, they are thought to differentiate

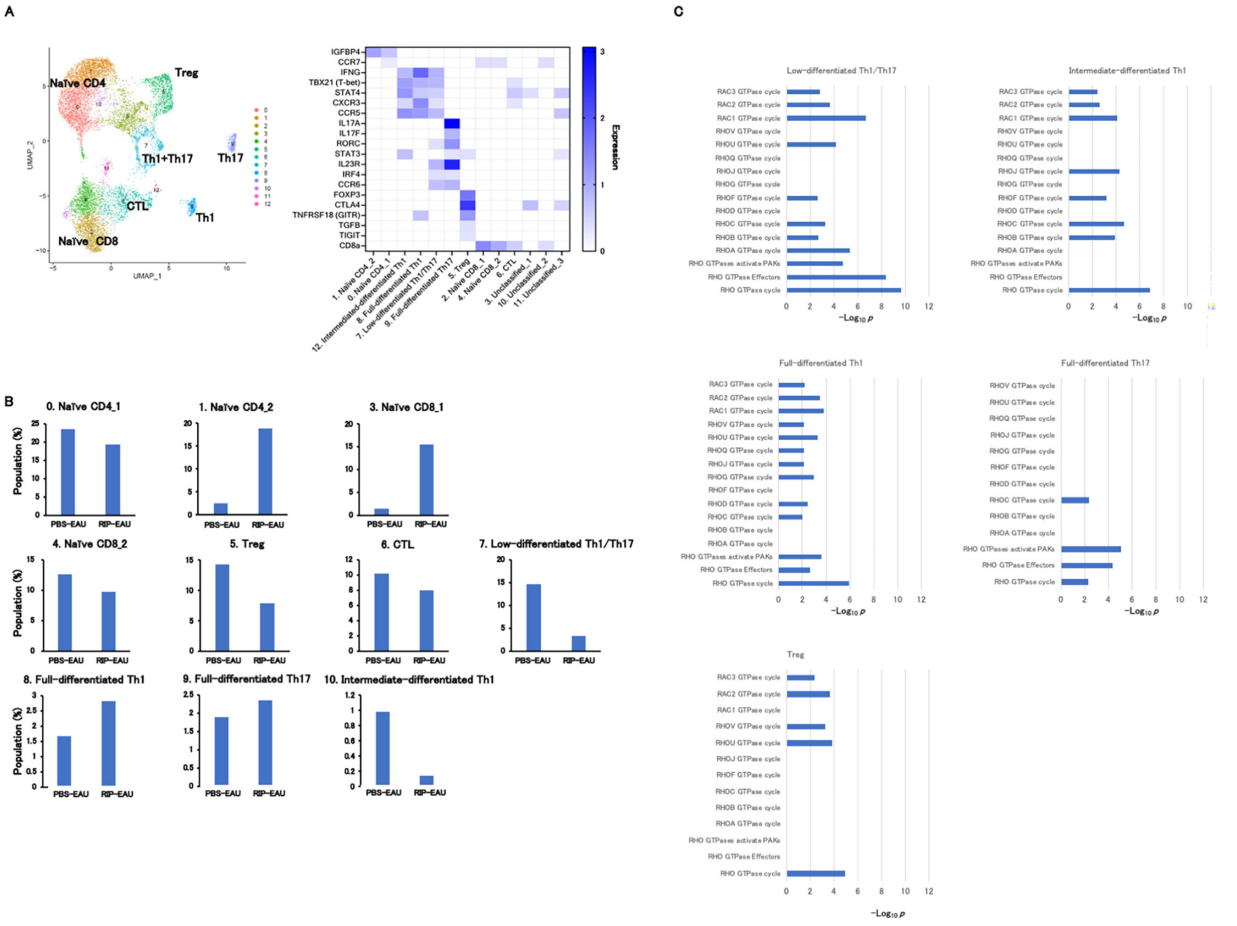

Figure 5 Identification of transcriptional changes associated with PBS-EAU and RIP-EAU mice by scRNA-seq (A) UMAP clustering plot of whole CD3$^+$ cells obtained from PBS-EAU and RIP-EAU mice annotated by immune cell marker gene expression and a heatmap showing immune cell marker gene expression in individual clusters. (B) Bar graphs showing the proportion of immune cell types in individual clusters. (C) Pathway enrichment analysis associated with highly expressed genes specific to individual clusters. RIP-EAU, ripasudil-experimental autoimmune uveoretinitis; UMAP, uniform manifold approximation and projection.

earlier than Th1 cells in the EAU model induced by hIRBP-p immunisation. In this study, ripasudil administration was initiated from the onset of EAU, suggesting that many cells destined to differentiate into Th17 cells may have already undergone differentiation before ripasudil treatment initiation. Therefore, the lack of suppression of IL-17-producing cells observed in RIP-EAU mice by FACS analysis could be attributed to the timing of ripasudil administration.

Drug repositioning is the process of finding an effective drug for one disease from an existing therapeutic drug for another disease and can significantly reduce the time and cost required for development compared with drug discovery. Ripasudil is already used as an eye drop to treat glaucoma. Our current findings show that ripasudil can suppress the progression of ocular inflammation even when administered during the effector phase of EAU, suggesting the potential of ripasudil through drug repositioning in the treatment of non-infectious uveitis.

Further investigations in this study are warranted to address the limitations of animal models, treatment protocols, mechanistic understanding and clinical translation. Specifically, studies in other animal species, evaluation of long-term treatment effects and dose optimisation, comprehensive analysis of ripasudil's impact on various immune cell types and signalling pathways and well-designed clinical trials are essential to fully validate the efficacy and safety of ripasudil for non-infectious uveitis treatment.

In conclusion, we demonstrated that ripasudil suppressed EAU development when administered from the onset of the disease. scRNA-seq analysis of T cells revealed that ripasudil specifically downregulated clusters of low-differentiated Th1/Th17 cells and intermediate-differentiated Th1 cells, which highly expressed genes involved in ROCK signalling pathway. These findings suggest that drug repositioning use of ripasudil could be a promising therapeutic agent for non-infectious uveitis. However, further studies are required to confirm the clinical efficacy and safety of ripasudil.

Acknowledgements The authors are grateful to Ms. Asami Taguchi for technical support with tissue section preparations and to Dr. Setsuko Mise for single cell RNA sequencing analysis.

Contributors KH, MI and MT made substantial contributions to the conception and design of the study. KH, YN and HS were responsible for data acquisition. KH and TS were responsible for data analysis. MI and MT for data interpretation. KH and MT wrote the main manuscript text. KH, YN, HS and MT revised the whole manuscript including all tables critically. MT is the guarantor. All authors approved the version to be published and agree to be accountable for all aspects of the work in ensuring that questions related to the accuracy or integrity of any part of the work are appropriately investigated and resolved.

Funding This work was supported by Grant-in-Aid for Scientific Research (23K09036).

Competing interests None declared.

Patient and public involvement Patients and/or the public were not involved in the design, or conduct, or reporting, or dissemination plans of this research.

Patient consent for publication Not applicable.

Ethics approval The study protocols were reviewed and approved by the Animal Ethics Committee of the National Defense Medical College (approval number: 19036), and the procedures were carried out according to the Association for Research in Vision and Ophthalmology Statement for the Use of Animals in Ophthalmic and Vision Research.

Provenance and peer review Not commissioned; externally peer reviewed.

Data availability statement Data are available on reasonable request. The datasets used and/or analysed during the current study are available from the corresponding author on reasonable request.

ORCID iD

Masaru Takeuchi http://orcid.org/0000-0002-4913-7089

REFERENCES

1 Williams GJ, Brannan S, Forrester JV, *et al*. The prevalence of sight-threatening uveitis in Scotland. *Br J Ophthalmol* 2007;91:33–6.
2 Jabs DA, Nussenblatt RB, Rosenbaum JT, *et al*. Standardization of uveitis nomenclature for reporting clinical data. Results of the First International Workshop. *Am J Ophthalmol* 2005;140:509–16.
3 Forrester JV, Kuffova L, Dick AD. Autoimmunity, Autoinflammation, and Infection in Uveitis. *Am J Ophthalmol* 2018;189:77–85.
4 Luger D, Silver PB, Tang J, *et al*. Either a Th17 or a Th1 effector response can drive autoimmunity: conditions of disease induction affect dominant effector category. *J Exp Med* 2008;205:799–810.
5 Agarwal RK, Horai R, Viley AM, *et al*. Abrogation of anti-retinal autoimmunity in IL-10 transgenic mice due to reduced T cell priming and inhibition of disease effector mechanisms. *J Immunol* 2008;180:5423–9.
6 Grajewski RS, Silver PB, Agarwal RK, *et al*. Endogenous IRBP can be dispensable for generation of natural CD4+CD25+ regulatory T cells that protect from IRBP-induced retinal autoimmunity. *J Exp Med* 2006;203:851–6.
7 Zhang L, Ma J, Takeuchi M, *et al*. Suppression of Experimental Autoimmune Uveoretinitis by Inducing Differentiation of Regulatory T Cells via Activation of Aryl Hydrocarbon Receptor. *Invest Ophthalmol Vis Sci* 2010;51:2109.
8 Lee DJ, Taylor AW. Both MC5r and A2Ar are required for protective regulatory immunity in the spleen of post-experimental autoimmune uveitis in mice. *J Immunol* 2013;191:4103–11.
9 Tybulewicz VLJ, Henderson RB. Rho family GTPases and their regulators in lymphocytes. *Nat Rev Immunol* 2009;9:630–44.
10 Riento K, Ridley AJ. Rocks: multifunctional kinases in cell behaviour. *Nat Rev Mol Cell Biol* 2003;4:446–56.
11 Biswas PS, Gupta S, Chang E, *et al*. Phosphorylation of IRF4 by ROCK2 regulates IL-17 and IL-21 production and the development of autoimmunity in mice. *J Clin Invest* 2010;120:3280–95.
12 Zanin-Zhorov A, Weiss JM, Nyuydzefe MS, *et al*. Selective oral ROCK2 inhibitor down-regulates IL-21 and IL-17 secretion in human T cells via STAT3-dependent mechanism. *Proc Natl Acad Sci U S A* 2014;111:16814–9.
13 Song J, Xi J-Y, Yu W-B, *et al*. Inhibition of ROCK activity regulates the balance of Th1, Th17 and Treg cells in myasthenia gravis. *Clin Immunol* 2019;203:142–53.
14 Sun X, Minohara M, Kikuchi H, *et al*. The selective Rho-kinase inhibitor Fasudil is protective and therapeutic in experimental autoimmune encephalomyelitis. *J Neuroimmunol* 2006;180:126–34.
15 Chen F, Hu H-H, Zhu J, *et al*. Removing the Retained Subfoveal Perfluorocarbon Liquid With Peeled Internal Limiting Membrane Reposition and Flute Aspiration. *Retina* 2022;42:1612–5.
16 Garnock-Jones KP. Ripasudil: first global approval. *Drugs (Abingdon Engl)* 2014;74:2211–5.
17 Uchida T, Honjo M, Yamagishi R, *et al*. The Anti-Inflammatory Effect of Ripasudil (K-115), a Rho Kinase (ROCK) Inhibitor, on Endotoxin-Induced Uveitis in Rats. *Invest Ophthalmol Vis Sci* 2017;58:5584–93.
18 Takeuchi M, Kezuka T, Sugita S, *et al*. Evaluation of the long-term efficacy and safety of infliximab treatment for uveitis in Behçet's disease: a multicenter study. *Ophthalmology* 2014;121:1877–84.
19 Mochizuki M, Nussenblatt RB, Kuwabara T, *et al*. Effects of cyclosporine and other immunosuppressive drugs on experimental autoimmune uveoretinitis in rats. *Invest Ophthalmol Vis Sci* 1985;26:226–32.
20 Harimoto K, Ito M, Karasawa Y, *et al*. Evaluation of mouse experimental autoimmune uveoretinitis by spectral domain optical coherence tomography. *Br J Ophthalmol* 2014;98:808–12.
21 Hao Y, Hao S, Andersen-Nissen E, *et al*. Integrated analysis of multimodal single-cell data. *Cell* 2021;184:3573–87.
22 Keino H, Takeuchi M, Usui Y, *et al*. Supplementation of CD4+CD25+ regulatory T cells suppresses experimental autoimmune uveoretinitis. *Br J Ophthalmol* 2007;91:105–10.
23 Liu X, Gu C, Lv J, *et al*. Progesterone attenuates Th17-cell pathogenicity in autoimmune uveitis via Id2/Pim1 axis. *J Neuroinflammation* 2023;20:144.
24 Tibbitt CA, Stark JM, Martens L, *et al*. Single-Cell RNA Sequencing of the T Helper Cell Response to House Dust Mites Defines a Distinct Gene Expression Signature in Airway Th2 Cells. *Immunity* 2019;51:169–84.
25 Grajewski RS, Hansen AM, Agarwal RK, *et al*. Activation of invariant NKT cells ameliorates experimental ocular autoimmunity by a mechanism involving innate IFN-gamma production and dampening of the adaptive Th1 and Th17 responses. *J Immunol* 2008;181:4791–7.
26 Constantinescu CS, Farooqi N, O'Brien K, *et al*. Experimental autoimmune encephalomyelitis (EAE) as a model for multiple sclerosis (MS). *Br J Pharmacol* 2011;164:1079–106.
27 Chen C, Li Y, Zhang Q, *et al*. Fasudil regulates T cell responses through polarization of BV-2 cells in mice experimental autoimmune encephalomyelitis. *Acta Pharmacol Sin* 2014;35:1428–38.
28 Zhao Y-F, Zhang X, Ding Z-B, *et al*. The therapeutic potential of Rho kinase inhibitor fasudil derivative FaD-1 in experimental autoimmune encephalomyelitis. *J Mol Neurosci* 2015;55:725–32.